The Canadian Mineralogist
Vol. 32, pp. 105-110 (1994)

AN OCCURRENCE OF SECTORED BIREFRINGENCE IN ALMANDINE FROM THE GAGNON TERRANE, LABRADOR

DENNIS BROWN

Department of Geology, Royal Holloway, University of London, Egham, Surrey TW20 0EX, U.K.

ROGER A. MASON

Department of Earth Sciences, Memorial University of Newfoundland, St. John's, Newfoundland A1B 3X5

Abstract

Optical birefringence in garnet, though common in the grandite series, is not widely known in other species. An occurrence of birefrigent almandine garnet ($Alm_{0.79}Grs_{0.173}Prp_{0.024}Sps_{0.015}$) has been found in graphitic schists of the Gagnon Terrane, Grenville Front, southwestern Labrador. In sections cut parallel to the *X–Y* plane, these grains show sectored extinction, with an extinction angle $\gamma \wedge [110] = 2°$. Birefringence is estimated to be 0.004 to 0.006. These grains also display a pattern of inclusions of cylindrical quartz intergrowths of a type that has been previously described in garnet from graphitic schists in Norway. An X-ray-diffraction analysis indicates a slight departure of the almandine from cubic symmetry.

Keywords: almandine, garnet, birefringence, cellular inclusions of quartz, sectored extinction, Gagnon Terrane, Labrador.

Sommaire

La biréfringence optique dans le grenat, quoique assez répandue dans les membres de la série "grandite", demeure méconnue dans les autres compositions de grenat. Nous décrivons un exemple d'almandin ($Alm_{0.79}Grs_{0.173}Prp_{0.024}Sps_{0.015}$) pris d'un schiste graphitique du bloc de Gagnon, près du front de Grenville, dans le secteur sud-ouest du Labrador. Dans les sections parallèles au plan *X–Y*, les grains montrent une extinction en secteurs, avec un angle d'extinction $\gamma \wedge [110]$ de 2°. La biréfringence aurait une valeur entre 0.004 et 0.006. Ces grains possèdent des inclusions cylindriques de quartz semblables à celles décrites antérieurement dans le grenat provenant de schistes graphitiques norvégiens. Une analyse par diffraction X indique un léger écart de la symétrie cubique.

(Traduit par la Rédaction)

Mots-clés: grenat almandin, biréfringence, inclusions cellulaires de quartz, extinction en secteurs, bloc de Gagnon, Labrador.

Introduction

Garnet, with few exceptions, is considered to be the optically isotropic mineral *par excellence*. Exceptions include spessartine, which may be weakly birefringent, and the members of the ugrandite group, which commonly show marked birefringence. A rare example of birefringence in almandine-rich garnet was noted by Kano & Yashima (1976). An interesting aspect of this problem is that birefringent garnet, when examined morphologically and by X-ray diffraction, demonstrates a cubic symmetry. Thus, the determination of symmetry is technique-dependent and must be operationally defined.

In addition to birefringence, garnet may show a complex series of sector twins composed of 6, 12, or 24 pyramids with vertices meeting at the center of the crystal [see Deer *et al.* (1982) and Rice & Mitchell (1991) for an overview]. Further, Harker (1939), Andersen (1984), and Burton (1986) described grains of garnet in graphitic metapelites from northern Norway that show pyramidal sectors with an unusual radial pattern of cellular inclusions of quartz.

This short paper provides a sample description, together with data obtained by electron microprobe, X-ray diffraction, and scanning electron microscopy (SEM), of an occurrence of birefringent, sectored almandine garnet with cellular inclusions of quartz. The sample comes from middle- to upper-greenschist-facies graphitic, metavolcanic schist within the metamorphic fold–thrust belt of the Gagnon Terrane, Grenville Province (Brown *et al.* 1992), southwestern Labrador (Lat. 53°34′N, Long. 65°42′E).

Sample Description

The sample consists of a fine-grained matrix made up of graphite, quartz, biotite, and minor ilmenite, and garnet porphyroblasts. The porphyroblasts are rusty brown to deep red, euhedral, and typically 3–5 mm in diameter. In some instances, the garnet grains display a cruciform pattern of inclusions reminiscent of a "chiastolite cross" (a pattern of carbonaceous inclusions commonly seen in andalusite). In thin section, the matrix is nearly opaque owing to the high modal abundance of graphite (Fig. 1). Biotite commonly rims the garnet porphyroblasts. Back-scatter SEM imaging and reflected light microscopy show a well-developed foliation defined by matrix minerals, that both abuts and wraps around the garnet porphyroblasts, suggesting syndeformational growth of the porphyroblasts. SEM imaging failed to show any textural evidence of plastic deformation, or the presence of cleavage domes (cf. Rice & Mitchell 1991).

Cut parallel to the X–Y plane, the garnet crystals have six pyramidal sectors that meet in the center of the crystal, with the {111} crystallographic planes defining the sector boundaries (Fig. 2). In polarized light, all parts of each grain of garnet show a marked birefringence that displays sectored extinction (Fig. 1). The extinction angle is approximately $\gamma \wedge [110] = 2°$ (Fig. 2). The extinction position varies slightly within each sector, displaying lineage-type structures (Fig. 1) parallel to quartz inclusions of type II (see below for description of types of inclusions). Birefringence does not vary near sector boundaries. Sectors appear to be biaxial, with a $2V$ angle of approximately 90°. Birefringence is estimated to be between 0.004 to 0.006.

Sectors contain numerous elongate inclusions of quartz aligned perpendicular to, and at 45° to the (110) crystal face. Sectors are separated by an inclusion-rich sector boundary that typically broadens outward, trumpet-like. Inclusions are of type I and type II, in the

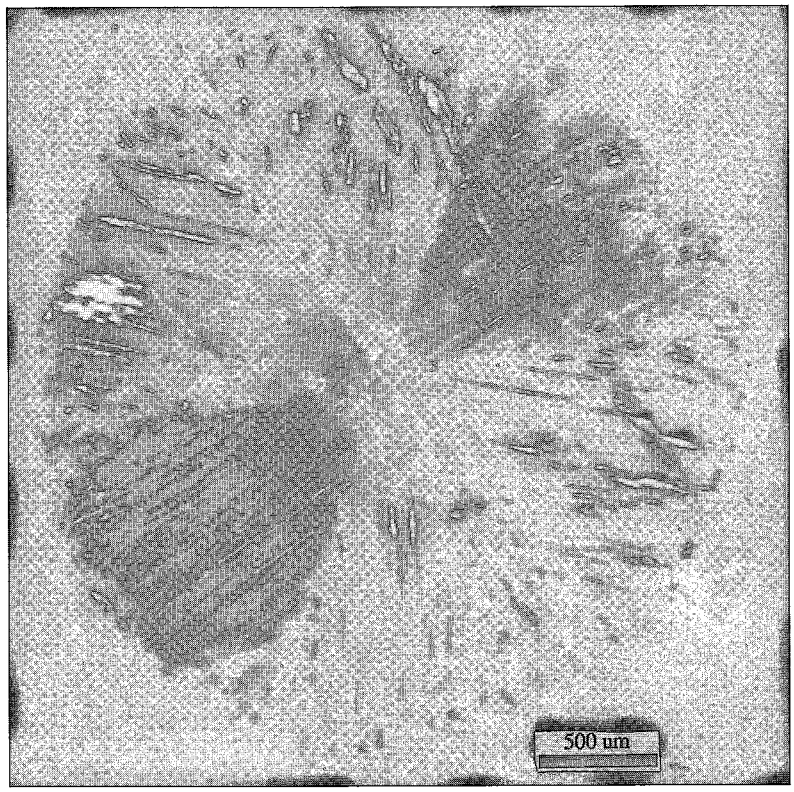

FIG. 1. Birefringent almandine garnet with sectored extinction. Type-I inclusions appear as equant grains along sector boundaries, and type-II inclusions are elongate and perpendicular to (110). Note the presence of lineage structures parallel to the type-II inclusions.

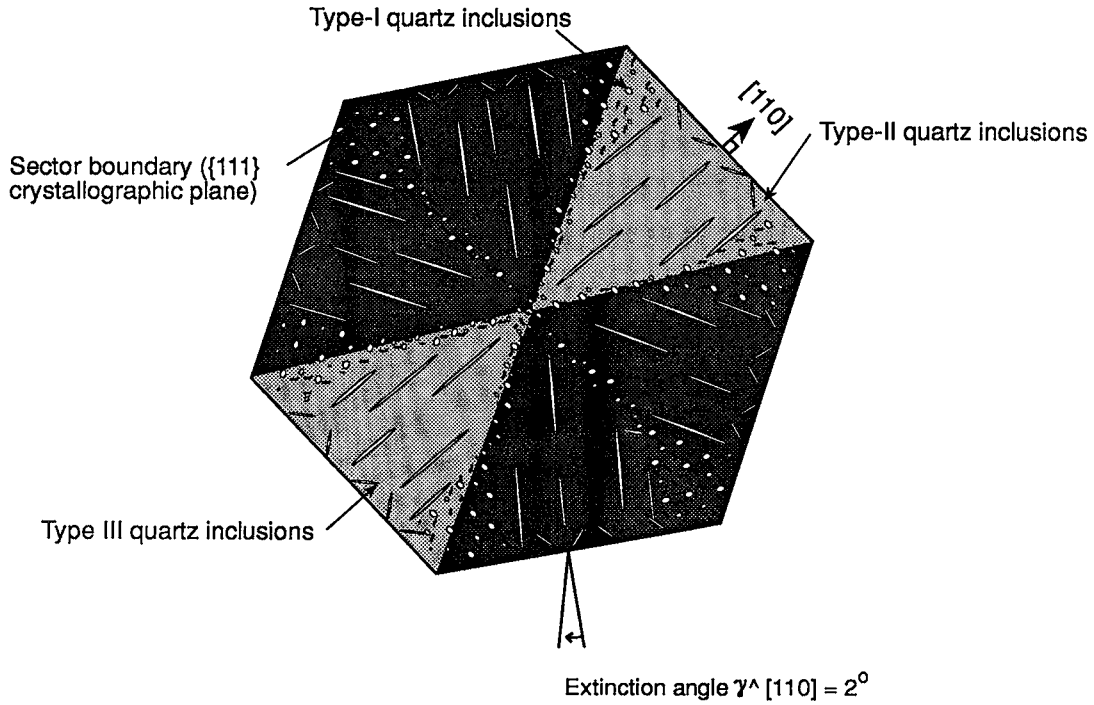

FIG. 2. Schematic illustration parallel to the *X–Y* plane, indicating the various types of inclusions and crystallographic planes and the extinction angle.

classification of Andersen (1984). A third pattern of inclusions is found in this example and is denoted type III.

Type-I inclusions consist of submillimetric, equant grains of quartz (elliptical in three dimensions), graphite, and ilmenite along sector boundaries, parallel to {111} crystallographic planes. Type-I inclusions are typically equigranular along the entire length of the sector boundary. Near the rim of the porphyroblasts, as the sector boundary opens out, type-I and type-II inclusions occur together. Sector boundaries end at the rim of the garnet with, commonly, a tuft of fine-grained ilmenite protruding beyond the (110) face, into the matrix.

Type-II inclusions consist of elongate, straight to slightly curved, cylindrical (prolate ellipsoid in three dimensions) quartz grains 10–50 μm in diameter and up to 1 mm in length. Type-II inclusions are oriented 90° to the (110) crystal face and are at an angle of 30° to the sector boundary (*i.e.*, {111}). Individual type-II inclusions typically have a uniform extinction, but within a sector, all type-II inclusions do not have the same extinction position. In sections cut perpendicular to the [110] direction, type-II inclusions have a circular to elliptical cross-section.

Type-III inclusions occur within sectors, commonly in the outer millimeter of the garnet (Fig. 2). These inclusions consist entirely of straight to tabular quartz, <10 μm in diameter and 100–200 μm long and oriented at 45° to {110}. Type-III inclusions generally cross-cut type-II inclusions. Like type-II inclusions, individual type-III inclusions have a uniform extinction, but each inclusion has a different position of extinction.

As pointed out by Andersen (1984) and Burton (1986), uniform extinction in type-II (and, here, type-III) inclusions indicates continuity of the crystal structure in each inclusion, but the absence of a preferred orientation suggests that interphase boundaries between quartz and garnet are noncoherent. Birefringent halos are not observed around the quartz inclusions.

Major-element analyses of garnet were carried out on a JEOL 50A electron microprobe. Traverses were made across grains from rim to rim, across sectors and on opposite sides of sector boundaries. All grains were found to consist predominantly of the almandine component ($Alm_{0.79}Grs_{0.173}Prp_{0.024}Sps_{0.015}$) (Table 1). The garnet shows typically continuous growth-related zonation, with the Mn content decreasing toward the rim and a concomitant increase in Fe content (results of core and rim analyses are shown in Table 1). Likewise, the Ca concentration decreases toward the rim, whereas Mg content increases. The pattern

TABLE 1. COMPOSITIONS OF SECTOR-ZONED ALMANDINE

	core	rim	core	rim	core	rim	core	rim
SiO_2	37.14	36.88	36.86	36.79	36.41	36.68	37.05	36.29
Al_2O_3	20.50	20.32	20.30	20.57	20.59	20.32	20.46	20.61
TiO_2	0.02	0.01	0.01	0.02	0.01	0.00	0.02	0.02
MgO	0.62	0.52	0.61	0.60	0.63	0.55	0.59	0.57
FeO	34.91	36.21	34.88	35.49	35.29	34.30	35.11	35.63
MnO	0.67	0.55	0.81	0.94	1.06	2.37	0.72	0.55
CaO	6.02	6.03	6.19	6.00	5.97	6.03	5.84	6.32
Cr_2O_3	0.04	0.02	0.00	0.03	0.04	0.00	0.01	0.05
Total	99.94	100.68	99.72	100.47	100.05	100.26	99.88	100.09
			Formula on the Basis of 12 Oxygens					
Si	2.99	3.00	3.00	2.96	2.97	2.99	2.99	2.94
Al	1.95	1.94	1.95	1.95	1.98	1.95	1.95	1.97
Ti	0.00	0.00	0.01	0.00	0.01	0.00	0.00	0.00
Mg	0.07	0.06	0.06	0.07	0.07	0.07	0.07	0.07
Fe	2.35	2.46	2.38	2.39	2.40	2.34	2.37	2.41
Mn	0.04	0.04	0.05	0.06	0.07	0.16	0.05	0.04
Ca	0.52	0.52	0.54	0.52	0.52	0.53	0.50	0.55
Cr	0.00	0.00	0.00	0.00	0.00	0.00	0.00	0.00
Total	7.94	8.03	8.01	7.97	8.03	8.03	7.96	7.99
			Mol % end-members					
X_{Alm}	0.787	0.798	0.783	0.786	0.783	0.755	0.792	0.788
X_{Prp}	0.024	0.020	0.020	0.023	0.024	0.022	0.023	0.021
X_{Grs}	0.173	0.169	0.178	0.170	0.169	0.170	0.168	0.178
X_{Sps}	0.015	0.012	0.018	0.020	0.023	0.053	0.015	0.012

* Analyses were done on a JEOL 50A electron microprobe with an accelerating voltage of 22 nanoamperes and a count rate of 60,000 per 30 seceonds. Data were corrected using ZAF corrections.

of growth zoning is continuous across sectors, and a uniform pattern of growth is present.

Grains were also probed radially, across sectors, to see if compositional sector-zoning (*cf.* Hollister 1970) occurs. The garnet grains examined in this study display no compositional sector-zonation, nor is there any compositional change within individual sectors.

Limited X-ray powder-diffraction analysis has been carried out using a Rigaku RU–200 unit. The pattern was corrected against Si metal, and all diffraction maxima generated by inclusions were identified before the unit-cell parameter was refined from 20 lines between 5° and 90° 2θ. Diffraction maxima are sharp and well resolved, with no extra reflections or peak broadening. However, detailed scans across the 400 reflection show that the reflection is split into two components, with essentially equal intensities (24% and 25% relative to the strongest line *versus* 40% for single 400 reflection given for almandine in the PDF file). No other reflection shows evidence of splitting. The unit-cell parameter is 1.1588 nm (standard error 0.0001 nm), a value consistent with the almandine-rich composition (Meagher 1982).

Discussion

Various proposals for the origin of birefringence in grandite-series garnet have been put forward, including: substitution of H_4 for Si, anisotropy due to residual strain in the structure, substitution of rare-earth elements and Ca in the *X* site, and ordering of Fe^{3+} and Al on octahedral sites, resulting in reduction of symmetry (see Allen & Buseck 1988, and references therein). Akizuki (1984), Allen & Buseck (1988), and Hatch & Griffen (1989) have suggested that perhaps the dominant mechanism resulting in birefringence in garnet is ordering of Fe^{3+} and Al on the octahedral site. Allen & Buseck (1988) further concluded that internal strain resulting from lattice mismatch also may cause a reduction in the symmetry of garnet, thereby producing birefringence.

Likewise, several theories have been proposed for the origin of the sectored pattern of inclusions described above. For instance, Harker (1939) attributed the pattern of inclusions to twinning under conditions of rapid growth. Andersen (1984) also suggested rapid growth, but attributed the pattern of inclusions to a mechanism involving the formation of cellular segments by a process involving screw dislocations, bounded by lineage structures along which the cellular inclusions of quartz formed. Burton (1986) suggested that under the conditions of metamorphism in the area he discussed (P 6.5 kbar, T 500°C), the solubility of SiO_2 will be significantly reduced in a CO_2-rich fluid as a result of a reduced fugacity of oxygen, thus restricting its transport *via* the fluid. This results in an excess of quartz at the site of garnet growth, which is incorporated into the growing garnet as cellular inclusions. Rice & Mitchell (1991) suggested that a displacement of matrix material during porphyroblast growth also may account for sector-zoning. We do not attempt to further elucidate the origin of the inclusions in this paper.

The preliminary results discussed in this paper show, unambiguously, almandine garnet with a marked birefringence (Fig. 1) and, in this instance, sectored extinction. The birefringence of the garnet suggests that the symmetry is lower than cubic. Takéuchi & Haga (1976), Akizuki (1984), and Allen & Buseck (1988) have determined orthorhombic, triclinic, and monoclinic symmetries for garnet of the grandite series. In the present samples, the reduced symmetry inferred from optical observations is manifested only poorly in the powder X-ray diffraction pattern. This problem is common to many descriptions of birefringent garnet. We suggest that the split

400 reflection indicates departure from cubic symmetry, but our data do not allow us to assign the garnet to a specific crystal-system.

The data obtained do not allow us to make any definitive statement regarding ordering of Fe^{3+} and Al on the octahedral site in the garnet. However, the abundance of graphite in the matrix, together with the analytical data in Table 1, strongly suggest that Fe^{3+} is likely to be a minor component. Therefore, any Fe^{3+}/Al order is unlikely to play a significant role in controlling the optical properties or X-ray-diffraction pattern.

Adams *et al.* (1975) and Rosenfeld (1969) suggested that birefrigent halos around quartz inclusions in garnet are the result of compressive stresses exerted on the host garnet by the inclusion. However, some of the observations of birefringence in the garnet discussed in this paper militate against the hypothesis that birefringence is caused by strain attendant upon incorporation of inclusions. For example, the X-ray-diffraction patterns show no sign of broadened diffraction-maxima, as would be expected in structurally distorted material. In addition, SEM studies provide no evidence of plastic deformation. However, the slight mismatch in lattice suggested by the lineage structures may indicate strain in the structure caused by the inclusions, suggesting that they may play an important role in the birefringence seen in the almandine from the Gagnon Terrane.

Although a direct causative link between birefringence and oriented inclusions may not exist, their association argues strongly that processes leading to the development of one also lead to the development of the other. Although the examples of garnet described by Harker (1939), Andersen (1984), and Burton (1986) do not show birefringence, the remarkable similarity in their morphology and occurrence (*i.e.*, in graphitic metapelites) to those in the material from the Grenville Province suggests that the stimulus for development of sectors, oriented inclusions, and birefringence lies in some peculiarity of the physicochemical conditions of garnet growth or subsequent thermal history. The identification of this stimulus and the structural mechanism of loss of symmetry must await further work.

Whatever the mechanisms of loss of symmetry, it is apparent that these grains display a marked sectored birefringence that strongly suggests twinning. Twinning in isometric minerals such as garnet, though rare, does occur. In the hexoctahedral class ($4/m\ 3\ 2/m$), to which garnet belongs, twinning typically occurs according to the Spinel Law (or dodecahedral twinning), with {111} as the twin plane and [111] as the twin axis. The sectored extinction described in this paper suggests that twinning may occur in almandine garnet, and the {111} plane, which bounds the sectors, may represent the twin plane.

ACKNOWLEDGEMENTS

Prof. R.A. Howie and J. Baker are thanked for reviewing an earlier draft of this manuscript. Comments by two anonymous reviewers, by L.S. Hollister, and by R.F. Martin improved the paper. R.M. acknowledges the receipt of an NSERC operating grant.

REFERENCES

ADAMS, H.G., COHEN, L.H. & ROSENFELD, J.L. (1975): Solid inclusion piezothermometry. II. Geometric basis, calibration for association quartz–garnet, and the application to some pelitic schists. *Am. Mineral.* **60**, 584-598.

AKIZUKI, M. (1984): Origin of optical variations in grossular – andradite garnet. *Am. Mineral.* **69**, 328-338.

ALLEN, F.M. & BUSECK, P.R. (1988): XRD, FTIR, and TEM studies of optically anisotropic grossular garnets. *Am. Mineral.* **73**, 568-584.

ANDERSEN, T.B. (1984): Inclusion patterns in zoned garnets from Magerøy, north Norway. *Mineral. Mag.* **48**, 21-26.

BROWN, D., RIVERS, T. & CALON, T. (1992): A structural analysis of a metamorphic fold–thrust belt, northeast Gagnon terrane, Grenville Province. *Can. J. Earth Sci.* **29**, 1915-1927.

BURTON, K.W. (1986): Garnet – quartz intergrowths in graphitic pelites: the role of the fluid phase. *Mineral. Mag.* **50**, 611-620.

DEER, W.A., HOWIE, R.A. & ZUSSMAN, J. (1982): *Rock-Forming Minerals.* **1A**. *Inosilicates.* Longman, London.

HARKER, A. (1939): *Metamorphism.* Methuen, London.

HATCH, D.M. & GRIFFEN, D.T. (1989): Phase transitions in the grandite garnets. *Am. Mineral.* **74**, 151-159.

HOLLISTER, L.S. (1970): Origin, mechanism, and consequences of compositional sector-zoning in staurolite. *Am. Mineral.* **55**, 742-766.

KANO, H. & YASHIMA, R. (1976): Almandine-garnets of acid magmatic origin from Yamanogawa, Fukushima Prefecture and Kamitazawa, Yamagata Prefecture. *J. Jap. Assoc. Mineral. Petrol. Econ. Geol.* **71**, 106-119.

MEAGHER, E.P. (1982): Silicate garnets. *In* Orthosilicates (P.H. Ribbe, ed.). *Rev. Mineral.* **5**, 25-66.

RICE, A.H.N. & MITCHELL, J.I. (1991): Porphyroblast textural sector-zoning and matrix displacement. *Mineral. Mag.* **55**, 379-396.

ROSENFELD, J.L. (1969): Stress effects around quartz inclusions in almandine and the piezothermometry of coexisting aluminum silicates. *Am. J. Sci.* **267**, 317-351.

TAKÉUCHI, Y. & HAGA, N. (1976): Optical anomaly and structure of silicate garnets. *Proc. Jap. Acad.* **52**, 228-231.

Received October 15, 1992, revised manuscript accepted February 16, 1993.